crystals

MDPI

Article

Catalyst-Free Synthesis of Novel 4-(Benzofuran-2-yl)-*N*-phenylthiazol-2(3*H*)-imines, Crystal Structure Elucidation, and the Effect of Phenyl Substitution on Crystal Packing

Bakr F. Abdel-Wahab [1], Benson M. Kariuki [2,*], Hanan A. Mohamed [1] and Gamal A. El-Hiti [3,*]

[1] Applied Organic Chemistry Department, Chemical Industries Research Institute, National Research Centre, Dokki, Giza 12622, Egypt; bf.fathy@nrc.sci.eg (B.F.A.-W.); ha.mostafa@nrc.sci.eg (H.A.M.)
[2] School of Chemistry, Cardiff University, Main Building, Park Place, Cardiff CF10 3AT, UK
[3] Department of Optometry, College of Applied Medical Sciences, King Saud University, Riyadh 11433, Saudi Arabia
* Correspondence: kariukib@cardiff.ac.uk (B.M.K.); gelhiti@ksu.edu.sa (G.A.E.-H.); Tel.: +966-11469-3778 (G.A.E.-H.); Fax: +966-11469-3536 (G.A.E.-H.)

Abstract: A one-pot reaction of an equimolar mixture of 4-methoxyaniline, phenyl isothiocyanate, and 2-bromoacetylbenzofuran in absolute ethanol in the absence of any catalysts afforded 4-(benzofuran-2-yl)-3-(4-methoxyphenyl)-*N*-phenylthiazol-2(3*H*)-imine with an 83% yield. Under similar conditions, 4-flouroaniline provided a mixture of the expected 4-(benzofuran-2-yl)-3-(4-fluorophenyl)-*N*-phenylthiazol-2(3*H*)-imine and unexpected 4-(benzofuran-2-yl)-*N*-(4-fluorophenyl)-3-phenylthiazol-2(3*H*)-imine at an overall 73% yield. The structures of the synthesized heterocycles were confirmed using NMR spectroscopy. The products were recrystallized from dimethylformamide to afford samples suitable for structural determination via single-crystal diffraction. The molecules of the products share a common backbone and have similar conformations. They also display some common intermolecular interactions, including C–H···X (X = N, O, π) and π···π contacts. The molecules differ due to the methoxy and fluoro substituents on their phenyl rings, resulting in variations in the extended network in the crystals. Electron density maps and Hirshfeld surfaces have been used to rationalize the intermolecular contacts.

Keywords: X-ray crystal structure; synthesis; 4-(benzofuran-2-yl)-3-(4-methoxyphenyl)-*N*-phenyl thiazol-2(3*H*)-imine; 4-(benzofuran-2-yl)-3-(4-fluorophenyl)-*N*-phenylthiazol-2(3*H*)-imine; 4-(benzofuran-2-yl)-*N*-(4-fluorophenyl)-3-phenylthiazol-2(3*H*)-imine

check for updates

Citation: Abdel-Wahab, B.F.; Kariuki, B.M.; Mohamed, H.A.; El-Hiti, G.A. Catalyst-Free Synthesis of Novel 4-(Benzofuran-2-yl)-*N*-phenylthiazol-2(3*H*)-imines, Crystal Structure Elucidation, and the Effect of Phenyl Substitution on Crystal Packing. *Crystals* **2023**, *13*, 1239. https://doi.org/10.3390/cryst13081239

Academic Editor: Alexander Y. Nazarenko

Received: 25 July 2023
Revised: 7 August 2023
Accepted: 9 August 2023
Published: 11 August 2023

Copyright: © 2023 by the authors. Licensee MDPI, Basel, Switzerland. This article is an open access article distributed under the terms and conditions of the Creative Commons Attribution (CC BY) license (https://creativecommons.org/licenses/by/4.0/).

1. Introduction

Heterocyclic compounds are used in many medical applications due to their various biological activities [1–3]. Among other reasons, heterocycles are attractive because of their amiability to molecular structure modification. In addition, their lipophilicity, solubility, polarity, and capacity for hydrogen bond formation can be manipulated to suit various applications. Consequently, heterocycles play a significant role in drug design and comprise most (85%) biologically active compounds [4]. The requirement for heterocycles for medicinal applications has increased the demand for the design and synthesis of new compounds. A range of heterocycles have exhibited antibacterial, antitumor, antifungal, and anti-inflammatory properties [5]. Nitrogen-based heterocycles are particularly compelling because of their potential in salient applications [6–10]. Notably, these compounds are found in natural products with unique pharmacological properties [11–13].

Heterocycles containing the thiazol-2-imine moiety are of interest for medicinal and agricultural uses [14–16]. The thiazole ring system is an essential core scaffold in many natural products; for example, it serves as a crucial component of penicillin and some of its derivatives. These compounds exhibit anticancer, antifungal, anti-inflammatory, kinase inhibition, plant growth regulation, insecticidal, and acaricidal properties [17–26].

Benzofurans are widely distributed in nature [27] and have been accredited with biodynamic and therapeutic qualities [28,29]. These compounds exhibit antibacterial, antitumor, antioxidant, antiparasitic, and anti-inflammatory properties [30–32]. The possible uses for these compounds have led to increased attention toward synthesizing heterocycles containing benzofuran [33–35]. The design, synthesis, and structural determination of heterocycles containing thiazole and benzofuran moieties (Figure 1) have been a focus of continued interest, and the characterization of related heterocycles has been reported [36–38].

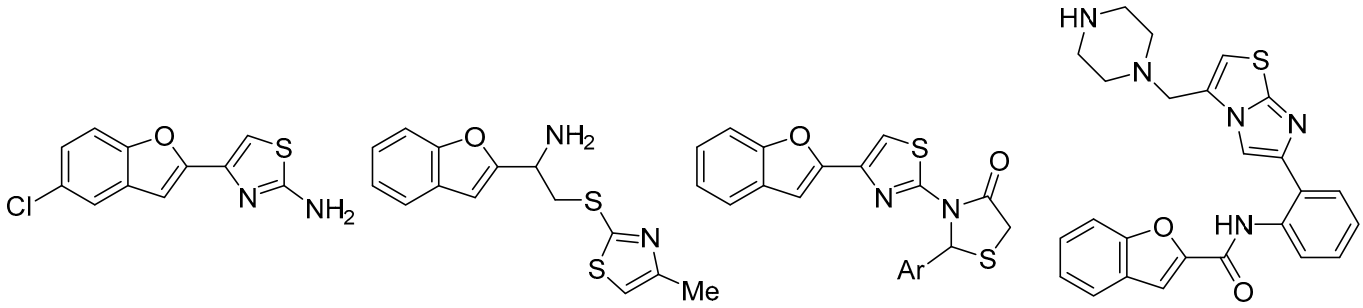

Figure 1. Important heterocycles containing thiazole and benzofuran moieties.

As part of our ongoing research into the design of heterocyclic molecules and the utilization of simple synthetic procedures, three new 4-(benzofuran-2-yl)-*N*-phenylthiazol-2(3*H*)-imines, namely, **5a**, **5b**, and **6**, that incorporate thiazole and benzofuran units have been obtained. Part of the work involved crystal structure characterization, enabling a detailed study of the intermolecular contacts in the solid state [39]. Molecules **5a**, **5b**, and **6** have a common backbone, and their crystal structures enable the exploration of the effect of different substituents on molecular packing in the solid state.

The understanding of molecular interactions in crystalline materials is fundamental to crystal engineering. The desired goal of crystal engineering is to understand intermolecular interaction leading to the eventual exploitation of this knowledge in designing and generating materials for specific functions [40–42]. The arrangement of molecules in the crystal structure depends on a combination of factors which include steric effects and electrostatic interactions. The shapes and sizes of molecules and substituents contribute significantly to determining their packing modes because of the need to maximize efficiency in the occupation of space [43]. The molecules under study do not possess strong hydrogen bond donors but can be involved in other types of contacts. Strong and weak hydrogen-bonding interactions [44], including those of the C–H···π type [45], are directional and have a structure-directing capacity in crystal structure formation. Other electrostatic interactions, including π···π [46] contacts, also contribute to structural direction and stabilization.

2. Materials and Methods

2.1. General

The chemicals, reagents, and solvents used in this study were purchased from Merck (Merck Life Science UK Limited, Gillingham, UK). The melting points of the synthesized heterocycles were determined using an electrothermal melting point apparatus (Cole-Parmer, Illinois, IL, USA). The IR spectra were recorded on a Bruker Tensor 27 FTIR spectrometer (Bruker, Tokyo, Japan). The NMR spectra (δ in ppm and *J* in Hz), recorded at 500 MHz for the proton and 125 MHz for the carbon measurements, were obtained in dimethyl sulfoxide (DMSO-d_6) using a JEOL NMR 500 MHz spectrometer (JEOL, Tokyo, Japan). The ^{19}F NMR spectrum was recorded on Bruker Avance III HD 400 spectrometer (Bruker, Tokyo, Japan). A CHNS-932 Vario elemental analyzer (LECO Instruments Ltd., Hazel Grove, Stockport, UK) was used to measure elemental content. Compound **4** was obtained from NRC-Fine Organic Chemicals Unit at the National Research Centre, Egypt. It was synthesized using a previously reported procedure [47].

2.2. Synthesis of 4-(Benzofuran-2-yl)-N-phenylthiazol-2(3H)-imines **5a** and a Mixture of **5b** and **6**

Scheme 1 shows the synthetic routes. A mixture of **1a** or **1b** (5 mmol) and **2** (5 mmol, 0.68 g) in dry EtOH (15 mL) was refluxed for 15 min, followed by the addition of **4** (5 mmol, 1.2 g). The reaction mixture was refluxed for four hours and then left to stand overnight. The resulting solid was filtered, dried, and recrystallized from DMF, yielding **5a** or a mixture of **5b** and **6**.

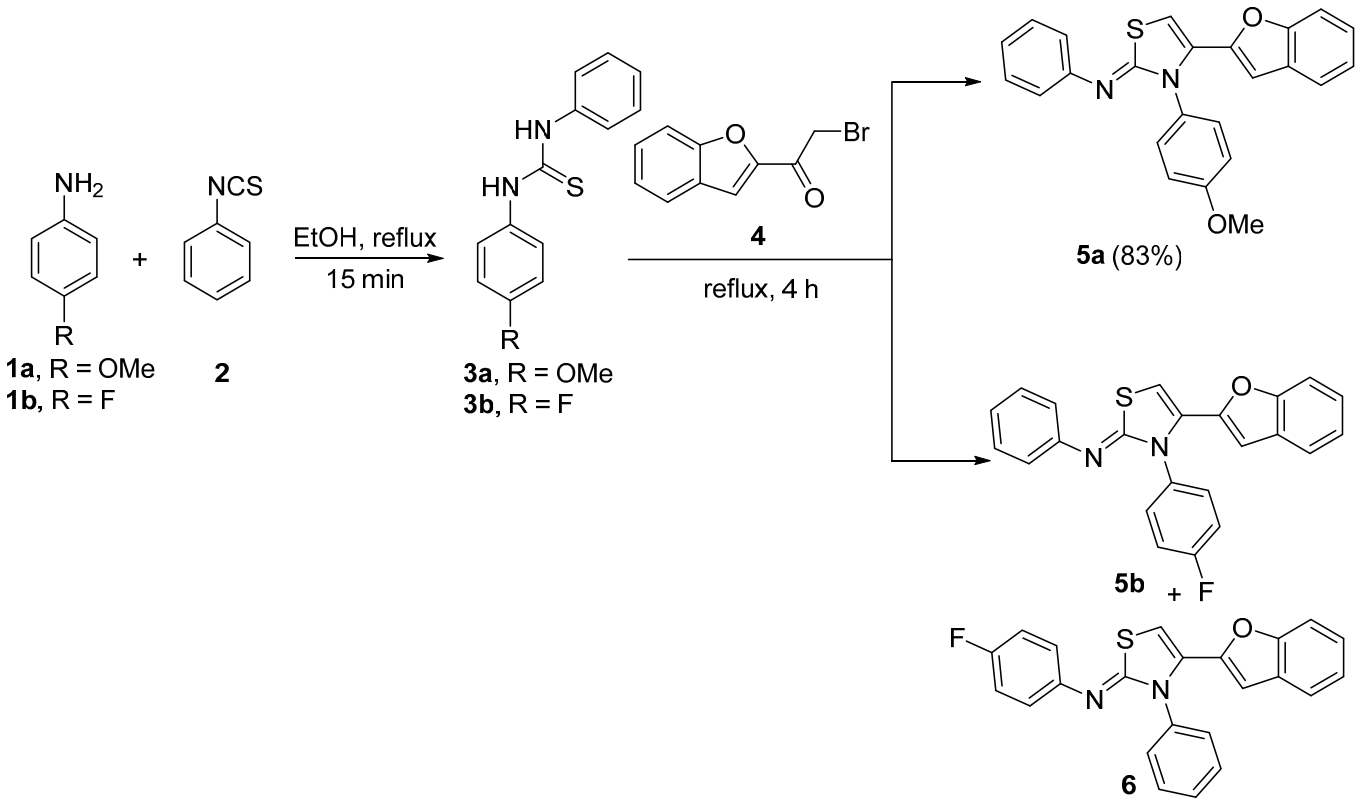

Scheme 1. Synthetic routes for the preparation of thiazol-2(3*H*)-imines **5a** and **b** and **6**. Equal amounts (5 mmol) of **1**, **2**, and **4** were used in boiling dry EtOH. The crystallization (DMF) of crude products resulted in **5a** (83%) and a mixture of **5b** and **6** (73%).

2.2.1. 4-(Benzofuran-2-yl)-3-(4-methoxyphenyl)-*N*-phenylthiazol-2(3*H*)-imine (**5a**)

Yield: 83%, mp 182–183 °C. IR (KBr): 3131 (CH), 1618 (C=N), and 1577 (C=C) cm^{-1}. ^{1}H NMR: 3.81 (s, 3H, OMe), 5.63 (s, 1H, thiazolyl), 6.87 (d, 7.7 Hz, 2H, Ar), 6.95 (s, 1H, Ar), 6.98 (t, 7.7 Hz, 1H, Ar), 7.07 (d, 8.6 Hz, 2H, Ar), 7.16 (t, 7.7 Hz, 1H, Ar), 7.27 (app t, 7.7 Hz, 3H, Ar), 7.39 (d, 8.6 Hz, 2H, Ar), and 7.48 (t, 7.7 Hz, 2H, Ar). ^{13}C NMR: 60.0, 100.4, 104.7, 111.3, 115.3, 121.4, 122.2, 123.6, 124.0, 126.0, 128.0, 130.1, 130.3, 130.7, 131.0, 146.5, 151.8, 153.9, 159.8, and 159.9. Anal. Calcd. for $C_{24}H_{18}N_2O_2S$ (398.46): C, 72.34; H, 4.55; N, 7.03. Found: C, 72.58; H, 5.09; N, 7.11%.

2.2.2. 4-(Benzofuran-2-yl)-3-(4-fluorophenyl)-*N*-phenylthiazol-2(3*H*)-imine (**5b**) and 4-(Benzofuran-2-yl)-*N*-(4-fluorophenyl)-3-phenylthiazol-2(3*H*)-imine (**6**)

Yield: 73%, mp 157–158 °C. IR (KBr): 3129 (CH), 1616 (C=N), and 1576 (C=C) cm^{-1}. ^{1}H NMR: 5.60, 5.74 (2 s, 2H, thiazolyl), 6.87–6.99 (m, 4H, Ar), 7.08–7.17 (m, 5 H, Ar), 7.25–7.29 (m, 5H, Ar), and 7.41–7.54 (m, 14H, Ar). ^{13}C NMR: 100.9, 101.0, 104.9, 105.1, 111.3, 116.6, 116.7, 116.9, 117.1, 121.4, 122.14, 122.3, 123.0, 123.0, 123.7, 123.7, 124.0, 126.1, 127.9, 128.0, 129.6, 129.8, 130.1, 132.0, 132.1, 134.4, 138.1, 146.2, 146.3, 148.2, 151.6, 153.9, 157.9, 159.9, 159.5, 159.8, 160.0, 161.4, and 163.3. ^{19}F NMR: 112.1, 120.4. Anal. Calcd. for $C_{23}H_{15}FN_2OS$ (386.43): C, 71.49; H, 3.91; N, 7.25. Found: C, 71.53; H, 4.08; N, 7.39%.

2.3. X-ray Crystal Structure

Diffraction data for **5a** and the mixed crystal of **5b** and **6** were recorded at 296 K on an Agilent SuperNova Dual Atlas single-crystal diffractometer with mirror-monochromated Mo radiation. Structure solution calculations were carried out using SHELXS [48] and refinement via SHELXL [49]. Anisotropic displacement parameters were utilized for non-hydrogen atoms during refinement. A riding model was used for hydrogen atoms with idealized geometry, and Uiso was set to 1.2 or 1.5 times the value of Ueq for the atom to which the hydrogen atoms were bonded. The para positions of the benzene rings in the molecule of **5b**/**6** were treated as disordered H/F with final occupancies of 0.332(4)/0.668(4) for F1/H15b and 0.668(4)/0.332(4) for F2/H21. The crystal and structure refinement data are shown in Table 1. The crystal structures of **5a** and **5b**/**6** have been deposited in the CSD under the reference numbers CCDC 2283522 and 2283523 (Supplementary Material).

Table 1. Crystal and structure refinement data of **5a** and the mixed crystal of **5b** and **6**.

Identification Code	5a	5b/6
Empirical formula	$C_{24}H_{18}N_2O_2S$	$C_{23}H_{15}FN_2OS$
Formula weight	398.46	386.43
T (K)	296(2)	293(2)
λ Å	0.71073	0.71073
Crystal system	Orthorhombic	Monoclinic
Space group	$P2_12_12_1$	$P2_1/c$
a (Å)	5.5731(5)	10.6289(9)
b (Å)	10.2520(9)	5.6010(3)
c (Å)	34.307(3)	30.567(2)
α (°)	90	90
β (°)	90	95.645(7)
γ (°)	90	90
Volume ($Å^3$)	1960.1(3)	1810.9(2)
Z	4	4
Density (calculated) (Mg/m^3)	1.350	1.417
Absorption coefficient (mm^{-1})	0.188	0.205
Crystal size (mm^3)	0.392 × 0.090 × 0.049	0.550 × 0.130 × 0.070
Reflections collected	16,408	15,447
Independent reflections	4878	4636
R(int)	0.0497	0.0539
Parameters	263	264
Goodness-of-fit on F2	1.055	1.059
R1 [I > 2σ(I)]	0.050	0.0584
wR2 [I > 2σ(I)]	0.0988	0.1076
R1	0.0843	0.1354
wR2	0.1143	0.1410
Largest diff. peak and hole ($e.Å^{-3}$)	0.195 and −0.214	0.206 and −0.255

2.4. Electrostatic Potentials and Hirshfeld Surface Calculations

The two components of the mixed crystal of **5b** and **6** were treated as independent ordered structures for the calculations. The input files for electrostatic potential calculation were prepared using Avogadro [50]. The electron density calculation was performed using the RHF/631G(dp) basis set in Gamess [51] and analyzed using Macmolplot [52]. The Hirshfeld surface was generated using CrystalExplorer17 [53].

3. Results and Discussion

A method that is frequently used for synthesizing thiazole ring systems is the reaction of haloketones with thioamides [54–56]. Other methods include the reaction of *N*,*N*-diformylaminomethyl aryl ketones with phosphorus pentasulfide in a basic medium [57] and the reaction of oximes and anhydrides with potassium thiocyanate and a copper catalyst [58]. Amines and aldehydes can also be used through a reaction with sulfur and

oxygen [59], while active methylene isocyanides and carbodithioates are synthesized with sodium hydride [60].

3.1. Synthesis of **5** *and* **6**

Thiazol-2-imines are commonly synthesized through a one-pot three-component reaction of aromatic α-bromoketones, primary amines, and phenyl isothiocyanate in ethanol (EtOH) in the presence of a catalytic amount of triethylamine [17,61]. In this study, two commercially available and easily accessible anilines, namely, 4-methoxyaniline (**1a**) and 4-flouroaniline (**1b**), were used. The procedure used resulted in high yields after optimization of the reaction conditions (including the solvent, time, and temperature). The progress of the reaction was observed using thin-layer chromatography. A one-pot reaction of equimolar amounts of **1a** (R = OMe), phenyl isothiocyanate (**2**), and then 2-bromoacetylbenzofuran (**4**) in dry ethanol (EtOH) afforded 4-(benzofuran-2-yl)-3-(4-methoxyphenyl)-*N*-phenylthiazol-2(3*H*)-imine (**5a**) at an 83% yield (Scheme 1). It should be noted that no catalysts were used. The reaction of **1b** (R = F), **2**, and **4**, under reaction conditions similar to those used for the production of **5a**, afforded the expected 4-(benzofuran-2-yl)-3-(4-fluorophenyl)-*N*-phenylthiazol-2(3*H*)-imine (**5b**) and the unexpected 4-(benzofuran-2-yl)-*N*-(4-fluorophenyl)-3-phenylthiazol-2(3*H*)-imine (**6**; Scheme 1) at a 73% overall yield as a 1:2 mixture. Several attempts were made to separate the two compounds through crystallization using different solvents, but these efforts were unsuccessful.

3.2. IR and NMR Spectroscopy of **5** *and* **6**

The chemical structures for **5a** and the mixture of **5b** and **6** were verified using IR, ^{1}H, and ^{13}C NMR spectroscopy (For further details, refer to the Supplementary Materials for the corresponding spectra.) In the IR spectra of **5a** (Figure S1) and the mixture containing **5b** and **6** (Figure S2), distinct absorption bands were observed at the 1616–1618 cm^{-1} and 1576–1577 cm^{-1} regions. These bands can be attributed to the stretching vibrations of the C=N and C=C groups, respectively. A distinct singlet signal was observed in the ^{1}H NMR spectrum of **5a** (Figures S3 and S4), indicating the presence of the thiazolyl proton at 5.63. In addition, the ^{1}H NMR spectrum of compound **5a** displayed a singlet signal at 3.80 ppm corresponding to the three protons from the OMe group. The ^{1}H NMR spectrum of the mixture containing **5b** and **6** (Figure S5) showed the thiazolyl proton at 5.75 and 5.60 ppm, respectively. Upon analyzing the ^{13}C NMR spectrum of **5a** (Figures S6–S8), it was confirmed that all carbons were detected at the anticipated locations following their chemical shifts. The ^{13}C NMR spectrum of the mixture containing **5b** and **6** (Figure S9) was complex and showed signals for both compounds. It was difficult to precisely determine the coupling constants between the carbon and fluorine atoms. The ^{19}F NMR spectrum of the mixture displayed two signals at 112.1 and 120.4, which corresponded to **5b** and **6**, respectively. Furthermore, there was indication of the existence of two additional minor isomers.

3.3. Proposed Mechanisms for the Formation of **5** *and* **6**

A proposed mechanism for the formation **5a** and **5b** is shown in Scheme 2. It involves the addition of **1a**,**b** to **2** to yield the corresponding thiourea **3a**,**b**. Thiourea **3a**,**b** tautomerizes to yield **7a**,**b** which reacts with 2-bromoacetylbenzofuran (**4**) to give the corresponding ketone **8a**,**b** and hydrobromic acid (HBr) as a side product. The tautomerization of **8a**,**b** yields **9a**,**b**, which loses H_2O to afford **5a**,**b**.

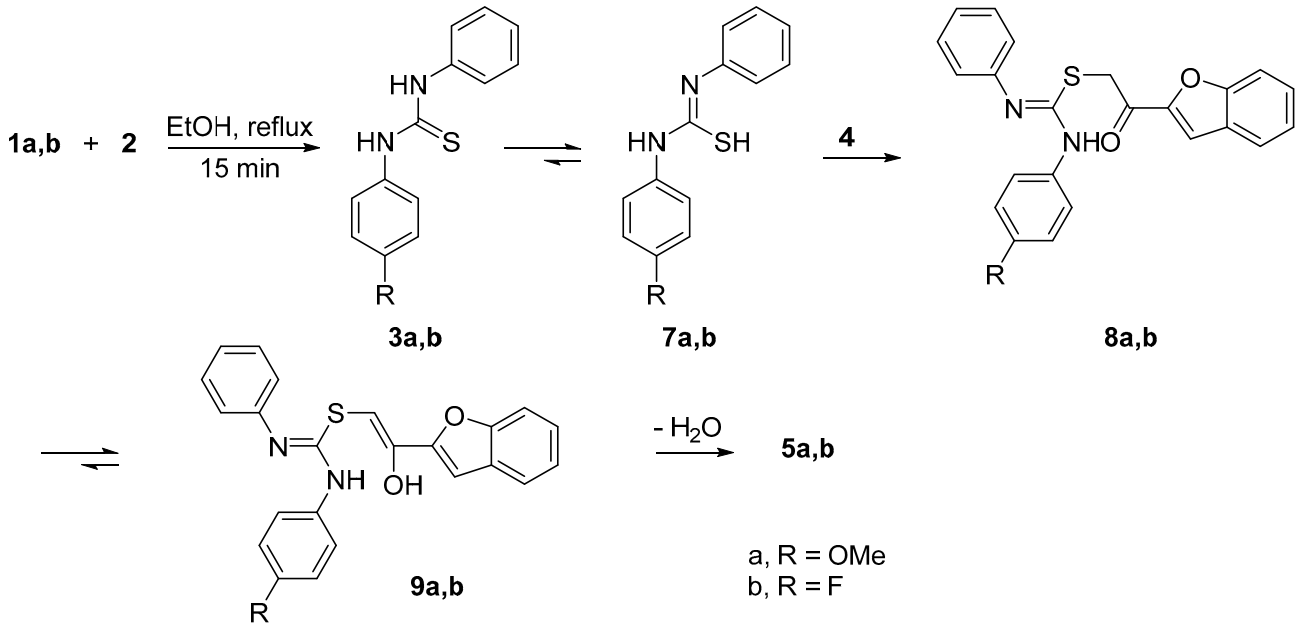

Scheme 2. A proposed mechanism for the formation of **5a** and **5b**.

The mechanism through which **6** is produced involves the addition of **1b** to **2** to yield thiourea **3b** (Scheme 3). The tautomerization of **3b** leads to the formation of **10** and **11,** which, on reaction with **4,** yield **12** and HBr as a side product. The tautomerization of **12** leads to **13,** which affords product **6** via the loss of H_2O (Scheme 3).

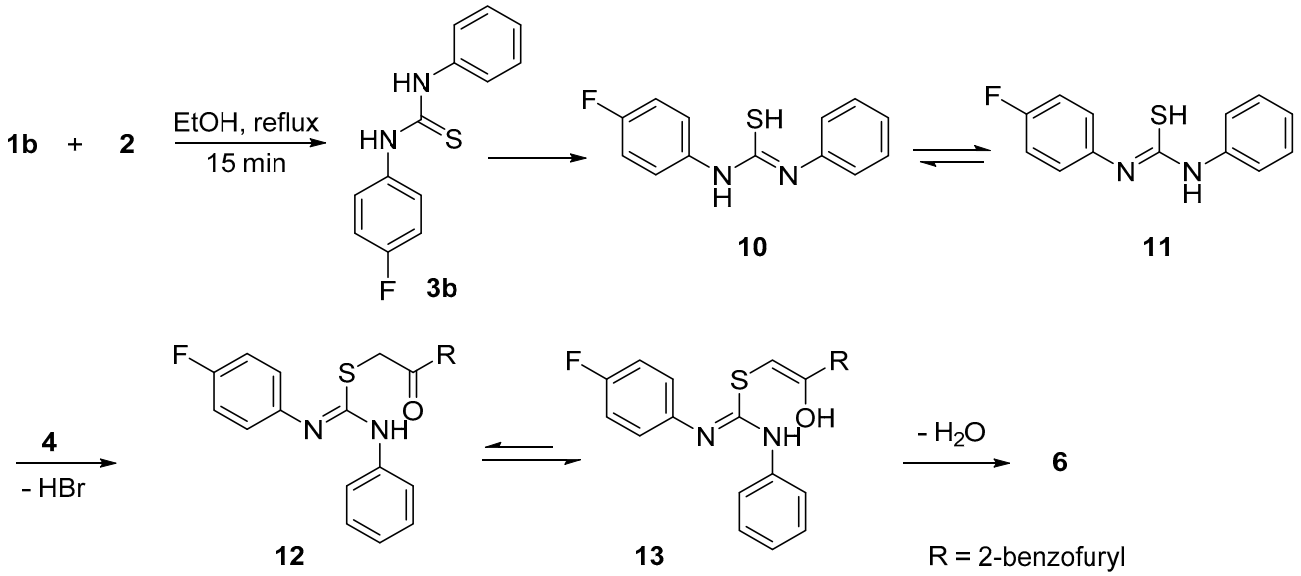

Scheme 3. A proposed mechanism for the formation of **6**.

3.4. X-ray Crystal Structures

3.4.1. Crystal Structure of **5a**

The crystal structure of **5a** is orthorhombic, space group $P2_12_12_1$, and an ortep representation of the molecule is shown in Figure 2a. The molecule comprises the following groups: benzofuran (**A**$_{5a}$, C1–C7, and O1), thiazole (**B**$_{5a}$, C9–C11, N1, and S1), methoxybenzene (**C**$_{5a}$, C12–C17, O2, and C24), and aminobenzene (**D**$_{5a}$, C18–C23, and N2). Rings **A**$_{5a}$ and **B**$_{5a}$ are almost co-planar in the molecule, with a twist angle **A**$_{5a}$/**B**$_{5a}$ of ca. 17°. In contrast, twist angles **B**$_{5a}$/**C**$_{5a}$ and **B**$_{5a}$/**D**$_{5a}$ are greater: they are in the range of 49–78° (Table 2).

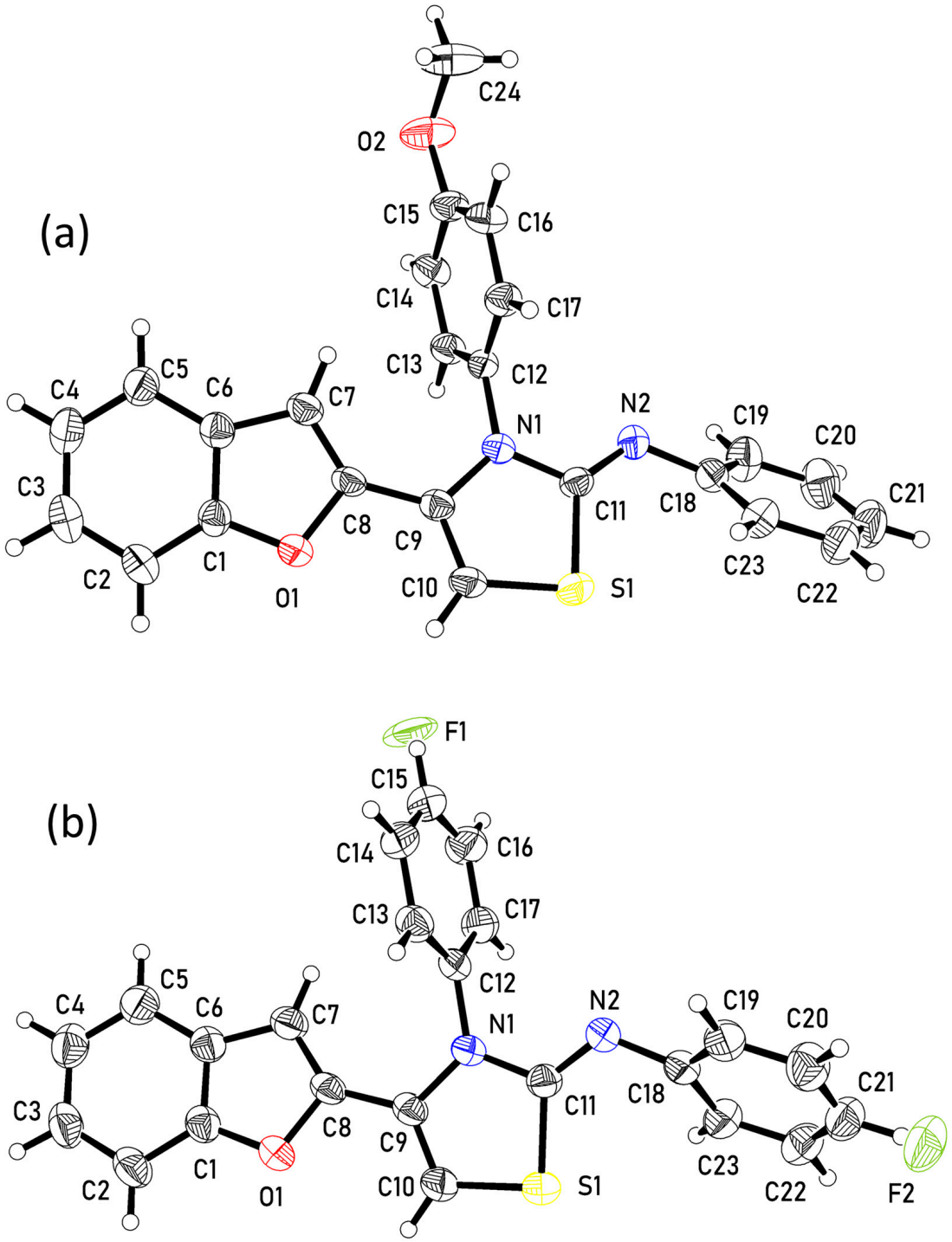

Figure 2. Ortep representation (at 50% probability atomic displacement parameters) for (**a**) **5a** and (**b**) the mixed crystal of **5b** and **6**. Both disorder components are shown for the mixed crystal.

Table 2. Group twist angles (°) for the molecule in the crystal structures of **5a** and the mixed crystal of **5b** and **6**.

	A/B	B/C	B/D
5a	16.98(16)	77.82(1)	49.55(12)
5b/6	17.55(12)	77.45(8)	54.51(8)

Molecule **5a** does not possess strong hydrogen bond donors, but its crystal structure displays weaker C–H···X (X = N, O) interactions (Table 3). In the crystal structure, C13–H13···N2 interactions (Figure 3a,b) between the methoxybenzene and aminobenzene groups of neighboring molecules form chains parallel to the direction of the a-axis. Within the chain, the furan group is involved in π–π contact with the thiazole group of a neighbor with a ring centroid-to-centroid distance of 3.93 Å (red dotted lines in Figure 3a,b).

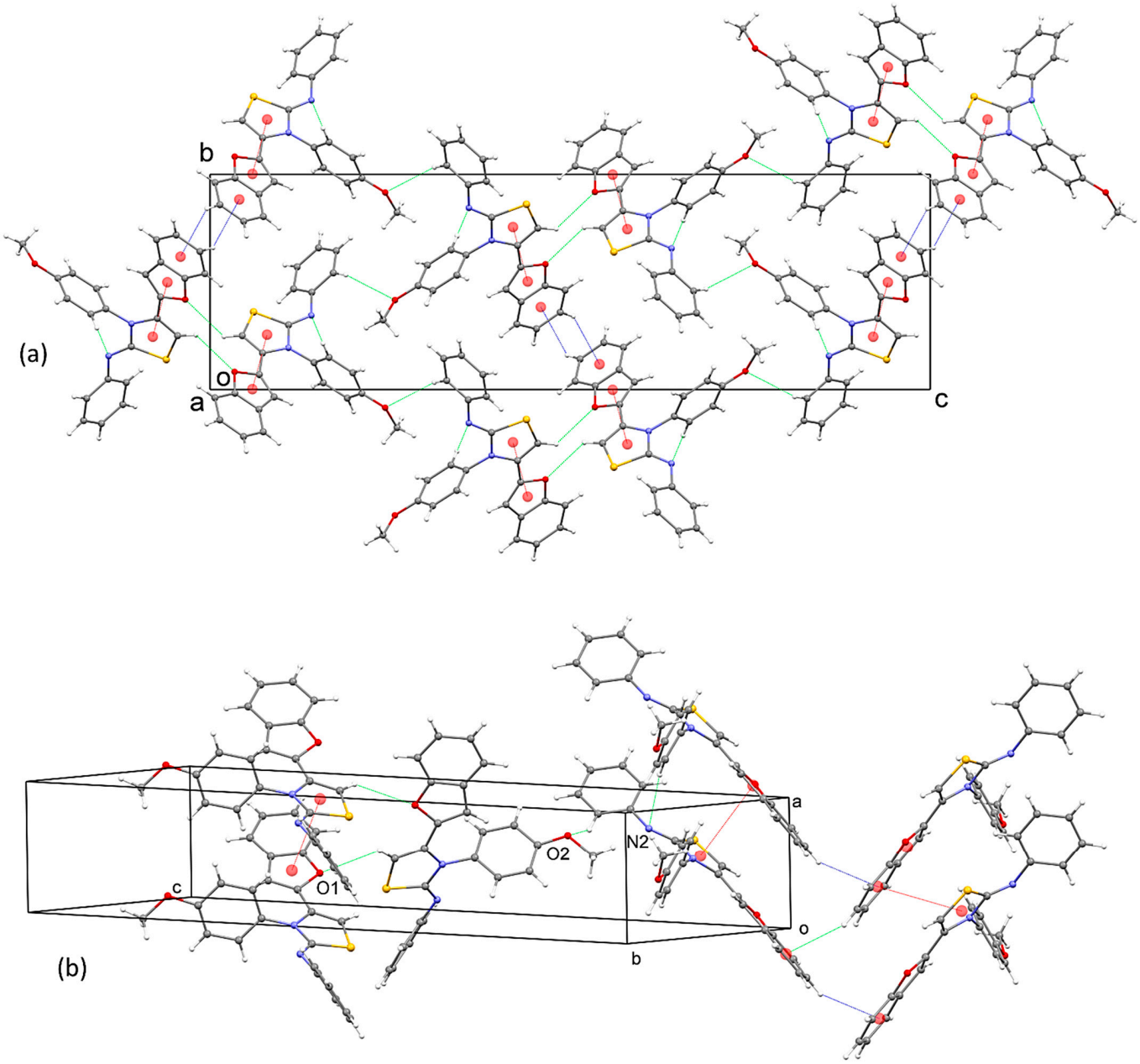

Figure 3. (**a**) The crystal packing in the structure of compound **5a**; (**b**) a segment of the structure. Intermolecular contacts are shown as dotted lines: green = C–H···N and C–H···O; blue = C–H···π; and red = π···π.

Table 3. Intermolecular contacts (Å, °) in the crystal structures of **5a** and the mixed crystal of **5b** and **6**.

		D···A	D–H···A
5a	C13–H13···N2	3.523(5)	162.8
	C10–H10···O1	3.280(4)	120.0
	C19–H19···O2	3.398(5)	136.3
5b/6	C13–H13···N2	3.634(3)	167.4
	C10–H10···O1	3.261(3)	117.2
	C7–H7···F2	3.392(4)	142.7
	C19–H19···F1	3.192(6)	156.1
	C2–H2···S1	3.812(3)	123.0

Each chain is linked to adjacent chains via the oxygen of the methoxybenzene group of a molecule accepting one C19–H19···O2 contact and the aminobenzene group donating another. The thiazole group also donates a C10–H10···O1 contact to a neighboring benzofuran group (shown in green in Figure 3a,b). Edge-to-face C–H···π contacts between the benzene rings of the benzofuran group with an H···ring centroid distance of 2.85 Å complete the extended 3D network in the structure (shown in blue in Figure 3a,b).

3.4.2. Structure of the Mixed Crystal of **5b** and **6**

Structure determination of the crystals obtained after synthesis showed that the substituents in the para positions of the phenyl rings were shared by H and F atoms, and this finding is consistent with the mixture of compounds obtained during synthesis (Scheme 1). The compounds were 4-(benzofuran-2-yl)-3-(4-fluorophenyl)-*N*-phenylthiazol-2(3*H*)-imine (**5b**) and 4-(benzofuran-2-yl)-*N*-(4-fluorophenyl)-3-phenylthiazol-2(3*H*)-imine (**6**), and the ratio of **5b**:**6** in the crystal was 0.33:0.67. Thus, the crystal structure contains a mixture of molecules **5b** and **6** with fluoro substituents on two different benzene rings. Despite the differences in the electronic properties of the benzene and fluorobenzene groups, solid solutions of compounds containing these groups can be formed due to the similar sizes of the groups, as observed in the case of benzoic acid and 4-fluorobenzoic acid [62].

The crystal structure of the mixed crystal of **5b** and **6** is monoclinic, space group $P2_1/c$, and an ortep representation of the asymmetric unit is shown in Figure 2b. The molecule consists of benzofuran (**A$_6$**, C1–C7, and O1), thiazole (**B$_6$**, C9–C11, N1, and S1), benzene/fluorobenzene (**C$_6$**, C12–C17, and F1), and aminobenzene/aminofluorobenzene (**D$_6$**, C18–C23, and F2) groups. In the molecule, the planes of rings **A$_6$** and **B$_6$** are close, with a twist angle **A$_6$**/**B$_6$** of ca. 18°, whereas twist angles **B$_6$**/**C$_6$** and **B$_6$**/**D$_6$** are in the range of 54–78° (Table 2).

As in the observation regarding the crystal structure of **5a**, C13–H13···N2 interactions (Figure 4a,b) between methoxybenzene and aminobenzene groups of neighboring molecules form chains parallel to the b-axis in the crystal of **5b**/**6**. The furan groups are also involved in π···π contact with the thiazole groups of neighboring molecules within the chain, with ring centroid-to-centroid distances of 3.99 Å.

Also, comparably with **5a**, the thiazole groups donate C10–H10···O1 interactions to neighboring benzofuran groups of adjacent chains (Table 3). Edge-to-face C–H···π connections between the benzene rings of the benzofuran groups with H···ring centroid distances of 2.98 Å are also observed (Figure 4a,b).

The chains are also linked through C–H···F interactions involving the aminofluorobenzene group. The group accepts a contact from the benzofuran group of a molecule from an adjoining chain and donates a contact to the fluorobenzene group of another chain. Interchain C2–H2···S1 contact also occurs.

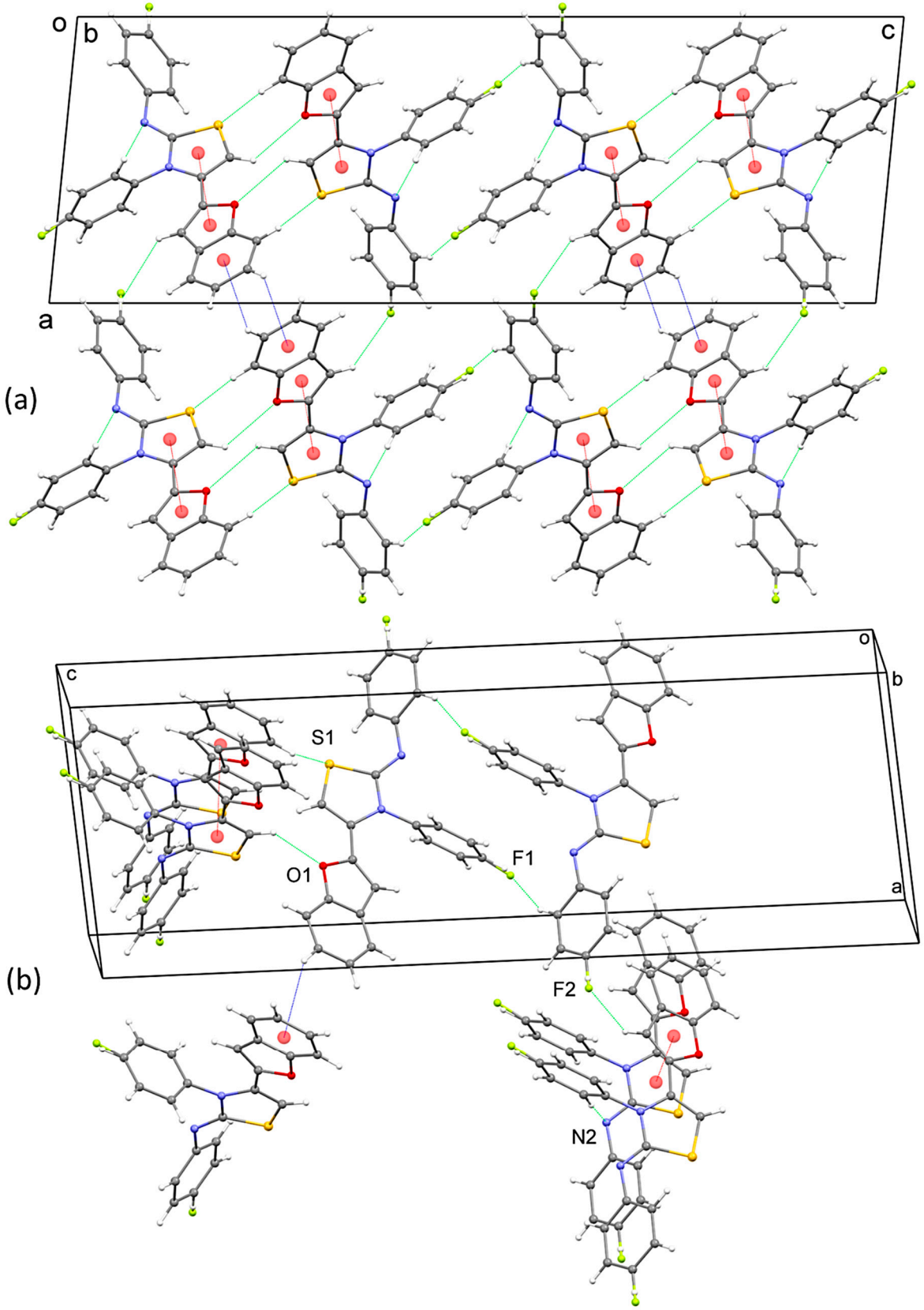

Figure 4. (**a**) Packing in the structure of the mixed crystal of compounds **5b** and **6** and (**b**) a segment of the structure. Intermolecular contacts are shown as dotted lines: green = C–H···N, C–H···O, C–H···S and C–H···F; blue = C–H···π; red = π···π.

3.4.3. Comparison of Crystal Packing

Generally, the arrangement of molecules in crystal packing depends on a combination of factors, including steric effects and electrostatic interaction. Steric effects influence molecular arrangement because the shapes and sizes of molecules and substituents largely determine the most efficient way the molecules can occupy space efficiently. The molecules of **5a**, **5b**, and **6** are identical, apart from the methoxy group in **5a** and the fluoro groups in **5b** and **6**. The similarity in the core of the molecules is reflected in the similarity in the twist angles between groups **A**/**B**, **B**/**C**, and **B**/**D** in the molecules (Table 2).

Electrostatic interactions, such as hydrogen bonding, may be directional and can thus steer molecules so that they pack in a specific way. It is noted here that there are no strong hydrogen bond donors in molecules **5a**, **5b**, and **6**. For ease of analysis and discussion, the two molecules in the mixed crystal of **5a** and **6** have been treated separately, retaining the packing obtained from the structural refinement of the mixed crystal structure.

The electron density isosurfaces for the molecules are shown in Figure 5. The positive regions, shown in red and clearly visible around the hydrogen atoms of the molecules, can donate weak hydrogen bonds. The negative regions, shown in blue, can accept hydrogen bonds. The main negative regions that are common to all the molecules are located on the benzofuran oxygen (O1) and the aminobenzene nitrogen (N2) atoms. Additionally, the methoxy oxygen in **5a** and the fluorine atoms in **5b** and **6** are negative.

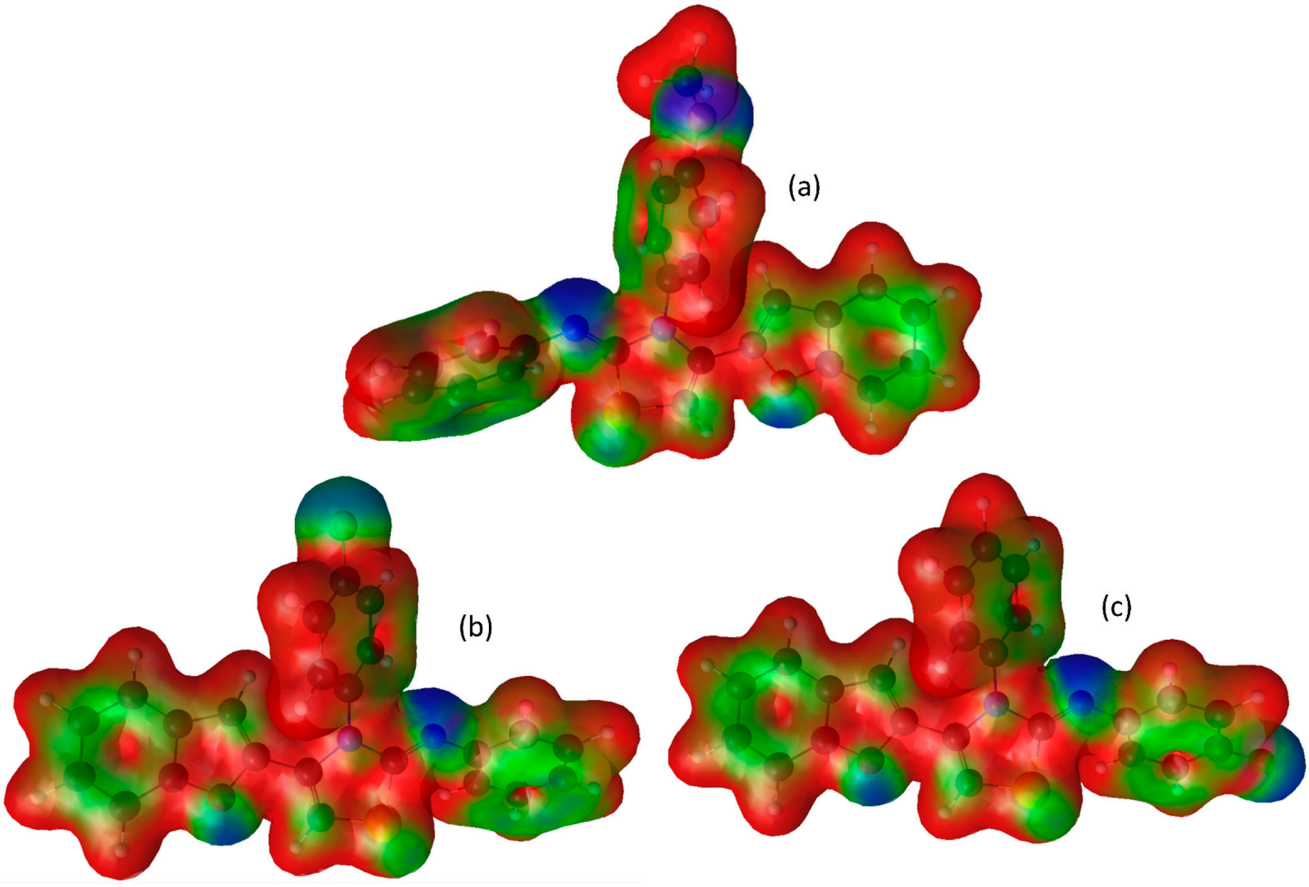

Figure 5. Electron density maps for molecules of (**a**) **5a**, (**b**) **5b,** and (**c**) **6**, with negative and positive regions represented in blue and red, respectively.

The segments that are common to molecules **5a**, **5b**, and **6** (i.e., all atoms except methoxy and F) participate in similar intermolecular interactions in the structures. The Hirshfeld surfaces, which show close contact between molecules, are presented in Figure 6. The distribution of the close contacts (highlighted in red) is similar for all the common parts of the molecules. As already discussed, the similar intermolecular contacts in the

structures involve C13–H13···N2 interactions between the benzene and aminobenzene groups of neighboring molecules, leading to the formation of chains, and the thiazole groups donating C10–H10···O1 contacts to neighboring benzofuran groups. Additionally, the furan groups are involved in π···π contact with the thiazole groups of neighboring molecules, and edge-to-face contacts between the benzene rings of the benzofuran groups also occur.

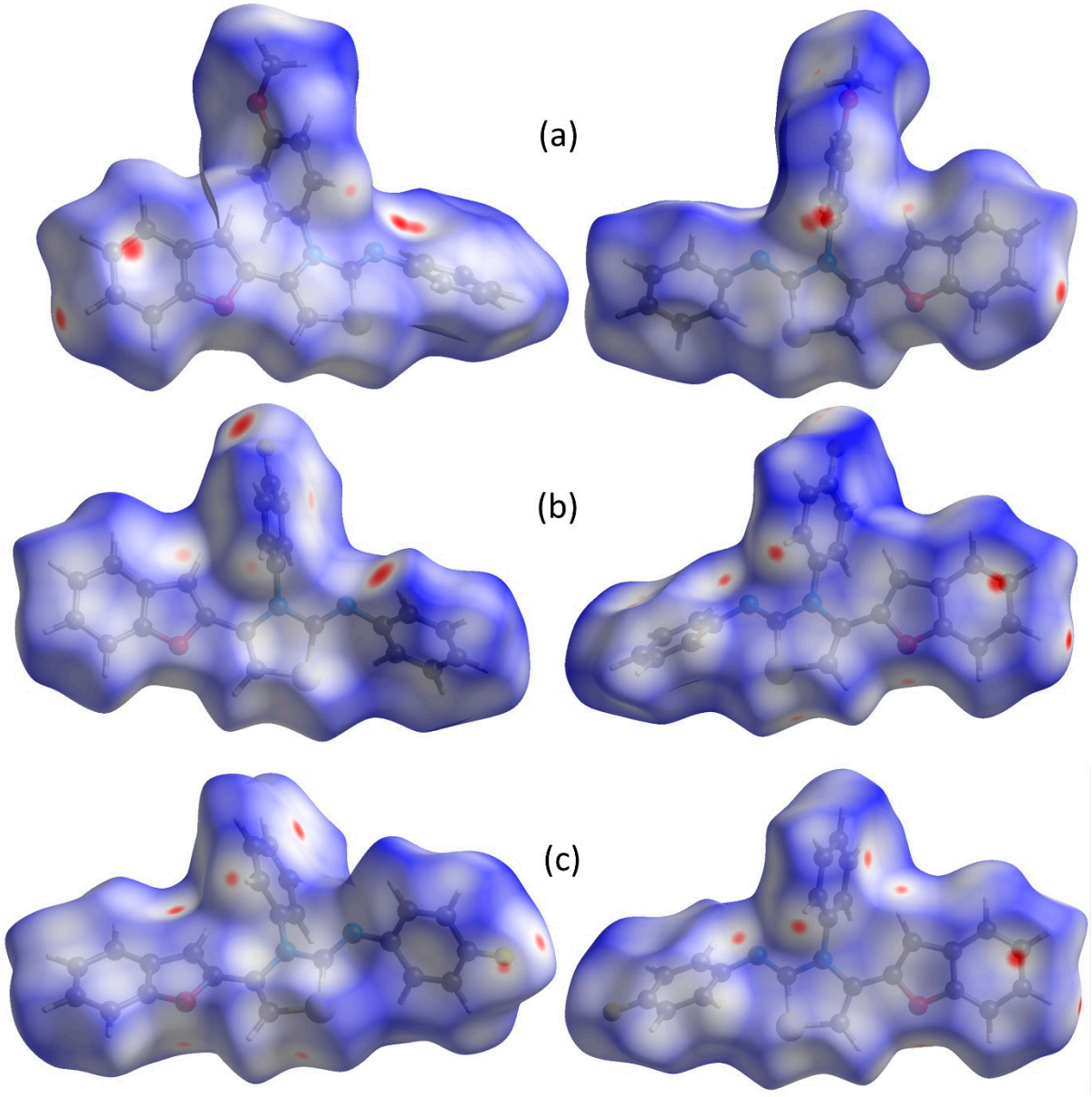

Figure 6. Hirshfeld surfaces for molecules (**a**) **5a**, (**b**) **5b,** and (**c**) **6** with areas of close intermolecular contact highlighted in red.

The electron density isosurfaces are negative for the regions around the methoxy oxygen and F atoms (the different substituents in **5a** and **5b**/**6**), and these atoms are involved in intermolecular hydrogen-bonding contact. Thus, the methoxybenzene group accepts a C19–H19···O2 interaction from an aminobenzene group, and C–H···F contacts are also observed for both the F atoms of molecules **5b** and **6** in the mixed crystal. Molecules **5a** and **5b** have methoxy and fluoro substituents, respectively, on the same benzene ring ($\mathbf{C_{5a}}$ and $\mathbf{C_6}$, respectively) and accept hydrogen bonds. However, it is observed that the

methyl on the methoxy group sterically hinders the oxygen atom and limits the direction of hydrogen bonding.

4. Conclusions

The successful synthesis of 4-(benzofuran-2-yl)-3-(4-methoxyphenyl)-*N*-phenylthiazol-2(3*H*)-imine in good yields was induced through one-pot reactions of an equimolar mixture of 4-methoxyaniline, phenyl isothiocyanate, and 2-bromoacetylbenzofuran in the absence of any catalysts. Under similar reaction conditions, the use of 4-fluroaniline led to the formation of a mixture of the expected 4-(benzofuran-2-yl)-3-(4-fluorophenyl)-*N*-phenylthiazol-2(3*H*)-imine and the unexpected 4-(benzofuran-2-yl)-*N*-(4-fluorophenyl)-3-phenylthiazol-2(3*H*)-imine. The structures of the newly synthesized heterocycles were determined using nuclear magnetic resonance spectroscopy and X-ray diffraction.

The crystal structures of **5a** and the mixed crystal of **5b** and **6** have been established. The identical segments of the molecules participate in similar intermolecular contacts of the C–H···N type between benzene and aminobenzene groups of neighboring molecules that result in the formation of chains, and thiazole groups donate C–H···O contacts to neighboring benzofuran groups. Furan groups are involved in π···π contact with the thiazole groups of neighboring molecules, and edge-to-face contacts occur between benzene rings of adjacent benzofuran groups. The different substituents, methoxy and fluorine, also accept C–H hydrogen-bonding contacts.

Supplementary Materials: The following supporting information can be downloaded at: https://www.mdpi.com/article/10.3390/cryst13081239/s1, Figure S1: IR spectrum of **5a**; Figure S2: IR spectrum for the mixture containing **5b** and **6**; Figure S3: ^{1}H NMR spectrum of **5a**; Figure S4: ^{1}H NMR spectrum (expansion) of **5a**; Figure S5: ^{1}H NMR spectrum for the mixture containing **5b** and **6**; Figure S6: ^{13}C NMR spectrum of **5a**; Figure S7: ^{13}C NMR spectrum (expansion) of **5a**; Figure S8: ^{13}C NMR spectrum (expansion) of **5a**; Figure S9: ^{13}C NMR spectrum for the mixture containing **5b** and **6**; Figure S10: ^{19}F NMR spectrum for the mixture containing **5b** and **6**; Figure S11: ^{19}F NMR spectrum for the mixture containing **5b** and **6**; Supplementary Files: SF1: CIF for **5a**, SF2: CIF for the mixed crystal of **5b** and **6**; SF3: CheckCIF report for **5a**; SF4: CheckCIF report for the mixed crystal of **5b** and **6**.

Author Contributions: Conceptualization: B.F.A.-W., B.M.K. and G.A.E.-H.; methodology: B.F.A.-W., H.A.M. and G.A.E.-H.; X-ray crystal structures: B.M.K.; investigation: B.M.K., B.F.A.-W., H.A.M. and G.A.E.-H.; writing—original draft preparation: B.F.A.-W., B.M.K. and G.A.E.-H.; writing—review and editing: B.F.A.-W., B.M.K. and G.A.E.-H. All authors have read and agreed to the published version of the manuscript.

Funding: G.A.E.-H. acknowledges the support from the Researchers Supporting Project (number RSP2023R404), King Saud University, Riyadh, Saudi Arabia.

Data Availability Statement: Data are contained within the article and the Supplementary Material.

Acknowledgments: We thank the National Research Centre and Cardiff University for technical support.

Conflicts of Interest: The authors have no conflict of interest to declare.

References

1. Kerru, N.; Gummidi, L.; Maddila, S.; Gangu, K.K.; Jonnalagadda, S.B. A review on recent advances in nitrogen-containing molecules and their biological applications. *Molecules* **2020**, *25*, 1909. [CrossRef] [PubMed]
2. Kabir, E.; Monir Uzzaman, M. A review on the biological and medicinal impact of heterocyclic compounds. *Results Chem.* **2022**, *4*, 100606. [CrossRef]
3. Amin, A.; Qadir, T.; Sharma, P.K.; Jeelani, I.; Abe, H. A review on the medicinal and industrial applications of N-containing heterocycles. *Open Med. Chem. J.* **2022**, *16*, 1–27. [CrossRef]
4. Jampilek, J. Heterocycles in medicinal chemistry. *Molecules* **2019**, *24*, 3839. [CrossRef] [PubMed]
5. Szumilak, M.; Stanczak, A. Cinnoline scaffold-A molecular heart of medicinal chemistry? *Molecules* **2019**, *24*, 2271. [CrossRef]
6. Kalaria, P.N.; Karad, S.C.; Raval, D.K. A review on diverse heterocyclic compounds as the privileged scaffold in antimalarial drug discovery. *Eur. J. Med. Chem.* **2018**, *158*, 917–936. [CrossRef] [PubMed]
7. Kerru, N.; Bhaskaruni, S.V.H.S.; Gummidi, L.; Maddila, S.N.; Maddila, S.; Jonnalagadda, S.B. Recent advances in heterogeneous catalysts for the synthesis of imidazole derivatives. *Synth. Commun.* **2019**, *49*, 2437–2459. [CrossRef]

8. Kerru, N.; Singh, P.; Koorbanally, N.; Raj, R.; Kumar, V. Recent advances (2015–2016) in anticancer hybrids. *Eur. J. Med. Chem.* **2017**, *142*, 179–212. [CrossRef]
9. Heravi, M.M.; Zadsirjan, V. Prescribed drugs containing nitrogen heterocycles: An overview. *RSC Adv.* **2020**, *10*, 44247–44311. [CrossRef]
10. Bellotti, P.; Koy, M.; Hopkinson, M.N.; Glorius, F. Recent advances in the chemistry and applications of *N*-heterocyclic carbenes. *Nat. Rev. Chem.* **2021**, *5*, 711–725. [CrossRef]
11. Kerru, N.; Maddila, S.; Jonnalagadda, S.B. Design of carbon–carbon and carbon–heteroatom bond formation reactions under green conditions. *Curr. Org. Chem.* **2019**, *23*, 3156–3192. [CrossRef]
12. Zarate, D.Z.; Aguilar, R.; Hernandez-Benitez, R.I.; Labarrios, E.M.; Delgado, F.; Tamariz, J. Synthesis of α-ketols by functionalization of captodative alkenes and divergent preparation of heterocycles and natural products. *Tetrahedron* **2015**, *71*, 6961–6978. [CrossRef]
13. Eftekhari-Sis, B.; Zirak, M.; Akbari, A. Arylglyoxals in synthesis of heterocyclic compounds. *Chem. Rev.* **2013**, *113*, 2958–3043. [CrossRef] [PubMed]
14. Chhabria, M.T.; Patel, S.; Modi, P.; Brahmkshatriya, P.S. Thiazole: A review on chemistry, synthesis and therapeutic importance of its derivatives. *Curr. Top. Med. Chem.* **2016**, *16*, 2841–2862. [CrossRef] [PubMed]
15. Nayak, S.; Gaonkar, S.L. A review on recent synthetic strategies and pharmacological importance of 1,3-thiazole derivatives. *Mini-Rev. Med. Chem.* **2019**, *19*, 215–238. [CrossRef]
16. Pawar, S.; Kumar, K.; Gupta, M.K.; Rawal, R.K. Synthetic and medicinal perspective of fused-thiazoles as anticancer agents. *Anticancer Agents Med. Chem.* **2021**, *21*, 1379–1402. [CrossRef] [PubMed]
17. Heravi, M.M.; Moghimi, S. An efficient synthesis of thiazol-2-imine derivatives via a one-pot, three-component reaction. *Tetrahedron Lett.* **2012**, *53*, 392–394. [CrossRef]
18. Nasiri, F.; Sabahi-Agabager, L. Efficient one-pot synthesis of thiazol-2-imine derivatives through regioselective reaction between primary amines, phenylisothiocyanate, and α-chloroacetaldehyde. *Comb. Chem. High Throughput Screen.* **2017**, *20*, 35–40. [CrossRef]
19. Singh, C.B.; Murru, S.; Kavala, V.; Patel, B.K. 3-Aryl-1-benzoylthioureas with a-bromoketones in water form 2-N-benzoyl-3-arylthiazol-2(3H)-imines, not 3-aryl-1-benzoylimidazoline-2-thiones. *J. Chem. Res.* **2007**, *2007*, 136–137. [CrossRef]
20. Dai, H.; Liu, J.; Zhang, X.; Yu, H.; Qin, X.; Qin, Z.; Wang, T.; Fang, J. Synthesis and biological activities of novel imine derivatives containing 2-substituted-1,3-thiazolidine and thiazole rings. *Chin. J. Org. Chem.* **2009**, *29*, 123–127.
21. Ramachandran, S.; Cheriyan, B.V.; Aanandhi, M.V. Activities of thiazolidine-4-one and azetidine-2-one derivatives—A review. *Res. J. Pharm. Tech.* **2021**, *14*, 4513–4516. [CrossRef]
22. Kumar, R.; Shuklab, A.; Tyagi, D.S. Synthesis of bioactive azetidinones of 4-phenyl-1,3-thiazole-2-amine. *Chem. Sci. Trans.* **2013**, *2*, 1518–1522. [CrossRef]
23. Yu, H.; Shao, L.; Fang, J. Synthesis and biological activity research of novel ferrocenyl-containing thiazole imine derivatives. *J. Organomet. Chem.* **2007**, *692*, 991–996. [CrossRef]
24. Sharma, P.C.; Bansal, K.K.; Sharma, A.; Sharma, D.; Deep, A. Thiazole-containing compounds as therapeutic targets for cancer therapy. *Eur. J. Med. Chem.* **2020**, *188*, 112016. [CrossRef]
25. Petrou, A.; Fesatidou, M.; Geronikaki, A. Thiazole ring-a biologically active scaffold. *Molecules* **2021**, *26*, 3166. [CrossRef]
26. Arshad, M.F.; Alam, A.; Alshammari, A.A.; Alhazza, M.B.; Alzimam, I.M.; Alam, M.A.; Mustafa, G.; Ansari, M.S.; Alotaibi, A.M.; Alotaibi, A.A.; et al. Thiazole: A versatile standalone moiety contributing to the development of various drugs and biologically active agents. *Molecules* **2022**, *27*, 3994. [CrossRef]
27. Miao, Y.H.; Hu, Y.-H.; Yang, J.; Liu, T.; Sun, J.; Wang, X.-J. Natural source, bioactivity and synthesis of benzofuran derivatives. *RSC Adv.* **2019**, *9*, 27510–27540. [CrossRef]
28. Khanam, H.; Shamsuzzaman. Bioactive Benzofuran derivatives: A review. *Eur. J. Med. Chem.* **2015**, *97*, 483–504. [CrossRef]
29. Metwally, M.A.; Abdel-Wahab, B.F.; El-Hiti, G.A. 2-Acetylbenzofurans: Synthesis, reactions and applications. *Curr. Org. Chem.* **2010**, *14*, 48–64. [CrossRef]
30. Nevagi, R.J.; Dighe, S.N.; Dighe, S.N. Biological and medicinal significance of benzofuran. *Eur. J. Med. Chem.* **2015**, *97*, 561–581. [CrossRef]
31. Abdel-Wahab, B.F.; Abdel-Aziz, H.A.; Ahmed, E.M. Convenient synthesis and antimicrobial activity of new 3-substituted 5-(benzofuran-2-yl)-pyrazole derivatives. *Arch. Pharm.* **2008**, *341*, 734–739. [CrossRef] [PubMed]
32. Abdel-Wahab, B.F.; Abdel-Aziz, H.A.; Ahmed, E.M. Synthesis and antimicrobial evaluation of 1-(benzofuran-2-yl)-4-nitro-3-arylbutan-1-ones and 3-(benzofuran-2-yl)-4,5-dihydro-5-aryl-1-[4-(aryl)-1,3-thiazol-2-yl]-1*H*-pyrazoles. *Eur. J. Med. Chem.* **2009**, *44*, 2632–2635. [CrossRef] [PubMed]
33. Baashen, M.A.; Abdel-Wahab, B.F.; El-Hiti, G.A. A simple procedure for the synthesis of novel 3-(benzofur-2-yl)pyrazole-based heterocycles. *Chem. Pap.* **2017**, *71*, 2159–2166. [CrossRef]
34. Pirouz, M.; Abaee, M.S.; Harris, P.; Mojtahedi, M.M. One-pot synthesis of benzofurans via heteroannulation of benzoquinones. *Synth. Commun.* **2021**, *27*, 24–31. [CrossRef]
35. Zhu, X.-R.; Deng, C.-L. Nickel-catalyzed intramolecular nucleophilic addition of aryl halides to aryl ketones for the synthesis of benzofuran derivatives. *Synthesis* **2021**, *53*, 1842–1848. [CrossRef]

36. Abdel-Wahab, B.F.; Bekheit, M.S.; Kariuki, B.M.; El-Hiti, G.A. (*E*)-*N*′-(1-(Benzofuran-2-yl)ethylidene)-1-(4-methoxyphenyl)-5-methyl-1*H*-1,2,3-triazole-4-carbohydrazide. *Molbank* **2023**, *2023*, M1657. [CrossRef]
37. El-Hiti, G.A.; Abdel-Wahab, B.F.; Baashen, M.; Ghabbour, H.A.; Alruqi, O.S. Crystal structure of 3-(benzofuran-2-yl)-5-(4-fluorophenyl)-4,5-dihydro-1*H*-pyrazole-1-carbothioamide, $C_{18}H_{14}FN_3OS$. *Z. Kristallogr. New Cryst. Struct.* **2016**, *231*, 887–888. [CrossRef]
38. El-Hiti, G.A.; Abdel-Wahab, B.F.; Hegazy, A.S.; Ajarim, M.D.; Kariuki, B.M. Crystal structure of 4-(benzofuran-2-yl)-2-(3-(4-fluorophenyl)-3,3*a*,4,5-tetrahydro-2*H*-benzo[*g*]indazol-2-yl)thiazole, $C_{28}H_{20}FN_3OS$. *Z. Kristallogr. New Cryst. Struct.* **2016**, *231*, 1171–1173. [CrossRef]
39. Kariuki, B.M.; Abdel-Wahab, B.F.; Bekheit, M.S.; El-Hiti, G.A. Intermolecular interactions of 3,5-bis(4-methoxyphenyl)-4,5-dihydro-1*H*-pyrazole-1-carbothioamide in a cocrystal with 1,3-*bis*(4-methoxyphenyl)prop-2-en-1-one and dimethylformamide solvate. *Crystals* **2022**, *12*, 663. [CrossRef]
40. Desiraju, G.R.; Vittal, J.J.; Ramanan, A. *Crystal Engineering: A Textbook*; IISc Press, World Scientific: Singapore, 2011.
41. Anthony, A.; Desiraju, G.R.; Jetti, R.K.R.; Kuduva, S.S.; Madhavi, N.N.L.; Nangia, A.; Thaimattam, R.; Thalladi, V.R. Crystal engineering: Some further strategies. *Cryst. Eng.* **1998**, *1*, 1–18. [CrossRef]
42. Braga, D. Crystal engineering, Where from? Where to? *Chem. Commun.* **2003**, *22*, 2751–2754. [CrossRef] [PubMed]
43. Kitaigorodskii, A. The principle of close packing and the condition of thermodynamic stability of organic crystals. *Acta Crystallogr.* **1965**, *18*, 585–590. [CrossRef]
44. Steiner, T. Reviews: The hydrogen bond in the solid state. *Angew. Chem. Int. Ed.* **2002**, *41*, 48–76. [CrossRef]
45. Nishio, M.; Umezawa, Y.; Fantini, J.; Weiss, M.S.; Chakrabarti, P. CH–π hydrogen bonds in biological macromolecules. *Phys. Chem. Chem. Phys.* **2014**, *16*, 12648–12683. [CrossRef] [PubMed]
46. Thakuria, R.; Nath, N.K.; Saha, B.K. The Nature and Applications of π–π Interactions: A Perspective. *Cryst. Growth Des.* **2019**, *19*, 523–528. [CrossRef]
47. Shriner, R.L.; Anderson, J. Derivatives of coumaran. VI. Reduction of 2-acetobenzofuran and its derivatives. *J. Am. Chem. Soc.* **1939**, *61*, 2705–2708. [CrossRef]
48. Sheldrick, G.M. A short history of SHELX. *Acta Cryst.* **2008**, *A64*, 112–122. [CrossRef] [PubMed]
49. Sheldrick, G.M. Crystal structure refinement with SHELXL. *Acta Cryst.* **2008**, *C71*, 3–8. [CrossRef]
50. Hanwell, M.D.; Curtis, D.E.; Lonie, D.C.; Vandermeersch, T.; Zurek, E.; Hutchison, G.R. Avogadro: An advanced semantic chemical editor, visualization, and analysis platform. *J. Cheminform.* **2012**, *4*, 17. [CrossRef]
51. Barca, G.M.J.; Bertoni, C.; Carrington, L.; Datta, D.; De Silva, N.; Deustua, J.E.; Fedorov, D.G.; Gour, J.R.; Gunina, A.O.; Guidez, E.; et al. Recent developments in the general atomic and molecular electronic structure system. *J. Chem. Phys.* **2020**, *152*, 154102. [CrossRef]
52. Bode, B.M.; Gordon, M.S. Macmolplt: A graphical user interface for GAMESS. *J. Mol. Graph. Model.* **1998**, *16*, 133–138. [CrossRef] [PubMed]
53. Spackman, P.R.; Turner, M.J.; McKinnon, J.J.; Wolff, S.K.; Grimwood, D.J.; Jayatilaka, D.; Spackman, M.A. CrystalExplorer: A program for Hirshfeld surface analysis, visualization and quantitative analysis of molecular crystals. *J. Appl. Crystallogr.* **2021**, *54*, 1006–1011. [CrossRef] [PubMed]
54. Ali, S.H.; Sayed, A.R. Review of the synthesis and biological activity of thiazoles. *Synth. Commun.* **2021**, *51*, 670–700. [CrossRef]
55. Byers, J.R.; Dickey, J.B. 2-Amino-4-methylthiazole. *Org. Synth.* **1939**, *19*, 10. [CrossRef]
56. Schwarz, G. 2,4-Dimethylthiazole. *Org. Synth.* **1945**, *25*, 35. [CrossRef]
57. Sheldrake, P.W.; Matteucci, M.; McDonald, E. Facile generation of a library of 5-aryl-2-arylsulfonyl-1,3-thiazoles. *Synlett* **2006**, 460–462. [CrossRef]
58. Tang, X.; Yang, J.; Zhu, Z.; Zheng, M.; Wu, W.; Jiang, H. Access to thiazole via copper-catalyzed [3+1+1]-type condensation reaction under redox-neutral conditions. *J. Org. Chem.* **2016**, *81*, 11461–11466. [CrossRef] [PubMed]
59. Wang, X.; Qiu, X.; Wei, J.; Liu, J.; Song, S.; Wang, W.; Jiao, N. Cu-Catalyzed aerobic oxidative sulfuration/annulation approach to thiazoles via multiple Csp3-H bond cleavage. *Org. Lett.* **2018**, *20*, 2632–2636. [CrossRef]
60. Lingaraju, G.S.; Swaroop, T.R.; Vinayaka, A.C.; Kumar, K.S.S.; Sadashiva, M.P.; Ragappa, K.S. An easy access to 4,5-disubstituted thiazoles via base-induced click reaction of active methylene isocyanides with methyl dithiocarboxylates. *Synthesis* **2012**, *44*, 1373–1379. [CrossRef]
61. Abdelfattah, A.M.; Sanad, S.M.H.; Ahmed, E.M.; Mekky, A.E.M. Regioselective synthesis and antibacterial screening of new thiazol-2(3H)-imines linked to arene or chromene units. *Synth. Commun.* **2023**, *53*, 1398–1411. [CrossRef]
62. Chakraborty, S.; Desiraju, G.R. C–H···F Hydrogen bonds in solid solutions of benzoic acid and 4-fluorobenzoic acid. *Cryst. Growth Des.* **2018**, *18*, 3607–3615. [CrossRef]

Disclaimer/Publisher's Note: The statements, opinions and data contained in all publications are solely those of the individual author(s) and contributor(s) and not of MDPI and/or the editor(s). MDPI and/or the editor(s) disclaim responsibility for any injury to people or property resulting from any ideas, methods, instructions or products referred to in the content.